

1 **Hemangiosarcoma cells induce M2 polarization and PD-L1 expression in macrophages**

2 Kevin Christian M. Gulay¹, Keisuke Aoshima^{1*}, Naoya Maekawa², Satoru Konnai^{2,3}, Atsushi

3 Kobayashi¹ & Takashi Kimura¹

4

5 ¹Laboratory of Comparative Pathology, Department of Clinical Sciences, Faculty of

6 Veterinary Medicine, Hokkaido University, Sapporo, Hokkaido, 060-0818, Japan.

7 ²Department of Advanced Pharmaceutics, Faculty of Veterinary Medicine, Hokkaido

8 University, Sapporo, Hokkaido, 060-0818, Japan.

9 ³Laboratory of Infectious Diseases, Department of Disease Control, Faculty of Veterinary

10 Medicine, Hokkaido University, Sapporo, Hokkaido, 060-0818, Japan.

11

12 **Keywords**

13 Hemangiosarcoma, M2 macrophages, PD-L1, syngeneic model, tumor microenvironment

14

15 **Corresponding author**

16 *Correspondence to Keisuke Aoshima, Laboratory of Comparative Pathology, Department of

17 Clinical Veterinary Sciences, Faculty of Veterinary Medicine, Hokkaido University, Kita 18

18 Nishi 9, Kita-ku, Sapporo, Hokkaido 060-0818, Japan: k-aoshima@vetmed.hokudai.ac.jp: Tel.

19 +81-11-706-5193

20

21 **Abstract**

22 Hemangiosarcoma (HSA) is a malignant tumor derived from endothelial cells.

23 Tumor-associated macrophages are one of the major components of tumor microenvironment

24 and crucial for cancer development. The presence and function of macrophages in HSA have

25 not been studied because there is no syngeneic model for HSA. In this study, we evaluated two

26 mouse HSA cell lines and one immortalized mouse endothelial cells for their usefulness as

27 syngeneic models for canine HSA. Our results show that the ISOS-1 cell line develops tumors

28 with similar morphology to canine HSA. ISOS-1 cells highly express KDM2B and have

29 similar KDM2B target expression patterns with canine HSA. Moreover, we determine that in

30 both ISOS-1 and canine HSA tumors, macrophages are present as a major constituent of the

31 tumor microenvironment. These macrophages are positive for CD204, an M2 macrophage

32 marker, and express PD-L1. ISOS-1-conditioned medium can induce M2 polarization and

33 PD-L1 expression in RAW264.7 mouse macrophage cell line. These results show that ISOS-1

34 can be used as a syngenic model for canine HSA and suggest that macrophages play an

35 important role in immune evasion in HSA. Using the syngeneic mouse model for canine HSA,

36 we can further study the role of immune cells in the pathology of HSA.

37

38 **Introduction**

39 Hemangiosarcoma (HSA) is a rapidly growing and highly invasive endothelial cancer¹.

40 It is the most common splenic neoplasm in dogs where it usually develops at 6 to 17 years of

41 age². Middle to large breed dogs are most commonly afflicted with HSA². HSA also occurs,

42 albeit infrequently, in cats, horses, mice, and humans³⁻⁶. An effective treatment for HSA is

43 difficult to develop since little is known about its molecular pathology. Recently, we found that

44 canine HSA highly expressed three histone demethylases (KDM1A, KDM2A and KDM2B)

45 out of which KDM2B was found necessary for HSA cell survival by positively regulating the

46 DNA damage response system in tumor cells⁷. KDM2B silencing not only dysregulated DNA

47 damage response but also induced expressions of the genes related to inflammatory responses⁷.

48 Inhibiting KDM2B could be an option to induce host immune responses against HSA tumor

49 cells. However, we were unable to investigate the function of KDM2B in canine HSA tumor

50 immune responses because the immunodeficient mouse model was not suitable to study the

51 immune responses⁸. Syngeneic mouse models, otherwise known as allograft mouse tumor

52 models, are composed of tumor tissues derived from the same genetic background as the

53 mouse strain. The syngeneic mouse models can develop tumors in a fully immunocompetent

54 environment, which can facilitate the examination of the immune-tumor cell interactions. A

55 syngeneic model for HSA, however, is non-existent.

56 At present, there are few established mouse HSA cell lines such as ISOS-1 and
57 UV♀2. ISOS-1 is a mouse HSA cell line established from a tumor formed by the
58 xenotransplantation of a human angiosarcoma cell line, while UV♀2 cell line is a mouse HSA
59 cell line developed from an ultraviolet light-induced HSA^{9,10}. Their usefulness as a syngeneic
60 model for canine HSA or human angiosarcoma, however, has not been evaluated.

61 Macrophages have two states, M1 and M2. M1 macrophages induced by
62 Lipopolysaccharides (LPS) and IFN γ are capable of killing tumor cells and presenting tumor
63 antigens to CD4⁺ T cells¹¹. M2 macrophages are polarized by IL-4, IL-10 and TGF β and are
64 important for tumor growth and immune evasion¹¹. They can produce anti-inflammatory
65 cytokines like IL-10, IL-3, and TGF- β which supports tumor development by repressing
66 cytotoxic T cell function^{12,13}. M2 macrophages in tumor tissues can be detected using CD204
67 (also known as MSR1) as a M2 macrophage marker¹⁴. *In vitro*, CD204 expression is induced
68 by TGF β treatment but LPS-treatment can also induce its expression via the MAPK/ERK
69 pathway in murine bone marrow-derived macrophages^{15,16}. It is highly likely that M2
70 macrophages support tumor development and facilitate immune evasion in HSA; however,
71 there are no studies that have evaluated their presence and functions in HSA.

72 In this study, we aimed to evaluate existing mouse HSA cell lines and immortalized

73 endothelial cells for their possible use as a syngenic model for canine HSA and to identify the
74 constituents of the tumor microenvironment and their roles in canine and mouse HSA
75 pathology.

76

77 **Results**

78 *ISOS-1 cells can be used as a syngenic model of canine HSA*

79 To find syngenic models for canine HSA, we first characterized two mouse
80 endothelial tumor cell lines: ISOS-1 and UV♀2, and one immortalized mouse endothelial cell
81 line, LEII. Morphologically, in single layer culture, both the mouse and canine HSA cell lines
82 are characterized by spindle to polygonal cells with a moderate amount of cytoplasm and
83 elongate nuclei arranged in cobblestone pattern (Fig. S1A). Then, we inoculated ISOS-1, LEII
84 and UV♀2 into Balb/c mice subcutaneously to determine their tumorigenic potential. All mice
85 inoculated with ISOS-1 cells developed tumors after 30 days post inoculation (dpi) and
86 reached the endpoint before 65 dpi (Fig. S1B). Mice inoculated with UV♀2 or LEII cells,
87 however, did not develop tumors. No metastasis was observed in ISOS-1 inoculated mice at
88 the endpoint. We then made histopathological sections of ISOS-1 tumors and compared their
89 morphologies with canine clinical HSA cases. ISOS-1 tumor cells formed variably sized,
90 irregular shaped blood vessels that were separated by thin septa and trabeculae. They showed

91 solid and capillary growth patterns which were also observed in canine HSA (Fig. 1A).
92 Spindle-shaped neoplastic endothelial cells line luminal spaces in a single layer and are plump,
93 hyperchromatic, and larger than normal endothelial cells (Fig. 1A, insets).

94 Next, we investigated whether ISOS-1, LEII and UV φ 2 have similar molecular
95 characteristics with canine HSA. Although *Kdm1a*, *Kdm2a* and *Kdm2b* gene expressions in the
96 mouse endothelial cell lines were not expressed more than 2-fold compared with primary
97 mouse lung endothelial cells (MLEC), their protein expressions in ISOS-1 were significantly
98 higher than in MLEC, LEII and UV φ 2 (Fig 1B and Fig. S2A). ISOS-1 tumor cells in Balb/c
99 mice also expressed KDM2B as high as in canine HSA (Fig 1C). Furthermore, ISOS-1 cells
100 had other similar molecular features to canine HSA cell lines such as cellular aneuploidy, low
101 p-ERK expression level and high c-FOS, γ H2A.X and H2AK119Ub1 expression levels (Figs.
102 1D - 1G).

103 Finally, we treated the mouse endothelial cell lines with GSK-J4, a histone
104 demethylase inhibitor, to know whether GSK-J4 can inhibit their viability and whether it is
105 more effective than doxorubicin like in canine HSA. The results showed that GSK-J4 could
106 inhibit the cell viability of ISOS-1, LEII and UV φ 2 at a lower IC₅₀ compared to doxorubicin
107 (Fig. S2).

108 These results demonstrate the numerous similarities between ISOS-1 cell line and

109 canine HSA, and they provide more proof of the usefulness of ISOS-1 as a syngeneic model
110 for canine HSA.

111

112 ***CD204⁺ macrophage is the major constituent in HSA tumor microenvironment***

113 To identify the constituent cells of the tumor microenvironment in HSA, we
114 immunohistochemically stained four ISOS-1 tumors developed in Balb/c mice and
115 twenty-eight clinical HSA samples in dogs with antibodies for Iba1 and CD3, a macrophage
116 and a T cell marker, respectively. T cells were present in minimal amount and were mostly
117 confined in the peripheries of tumor tissues. However, Iba1 staining revealed that
118 macrophages were the major components of tumor microenvironment in both ISOS-1 tumor
119 and canine HSA cases (Fig. 2A). The average percentages of macrophages in tumor tissues
120 were 65.27% and 48.83% in ISOS-1 tumors and canine HSA cases, respectively (Figs. 2B).

121 Next, to know whether HSA cells actively recruit macrophages, we performed
122 Transwell migration assay and compared the number of migrated macrophage-like RAW264.7
123 cells in conditioned media from MLEC or ISOS-1. As a result, the number of migrated
124 RAW264.7 cells significantly increased when cultured in conditioned medium from ISOS-1
125 compared to the conditioned medium from MLEC (Figs. 2C and 2D). RAW264.7 cells
126 cultured in ISOS-1 conditioned medium did not induce M1 macrophage-related genes but

127 highly expressed M2 macrophage markers such as *HAVCR2* and *CDI63* (Fig. 2E). The protein
128 expression of CD204, another M2 macrophage marker, was also induced by ISOS-1
129 conditioned medium in RAW264.7 cells. Lastly, we stained ISOS-1 tumors and canine HSA
130 cases with anti-CD204 antibody and identified a large number of CD204 positive cells in
131 ISOS-1 tumors and canine HSA samples (Fig. 2G)

132 These results suggest that HSA tumor cells recruit macrophages into the tumor
133 microenvironment and polarize them to M2 macrophages.

134

135 ***Tumor cells and tumor infiltrating macrophages express PD-L1 in HSA***

136 In both ISOS-1 tumor and canine HSA cases, macrophages dominate the tumor
137 parenchyma along with the tumor cells, thus, it is vital to know how these macrophages
138 contribute to HSA pathology. CD204⁺ macrophages in tumor tissues have been reported to
139 express PD-L1 and are associated with tumor malignancy and PD-L1 upregulation in tumor
140 and immune cells^{17,18}. Thus, we decided to examine PD-L1 expressions in tumor cells and
141 macrophages in clinical HSA cases and HSA cell lines.

142 PD-L1 was expressed in tumor cells and macrophages in 15 out of the 28 (53.6%)
143 and 19 out of the 28 (67.8%) canine HSA cases, respectively (Fig. 3A and Table). 23 out of 28
144 cases (82.1%) expressed PD-L1 in tumor cells and/or macrophages (Table). The PD-L1 signal

145 intensity in macrophages was stronger than that in ISOS-1 tumor cells. PD-L1 was also
146 expressed in ISOS-1 and canine HSA cell lines: JuB2, JuB4 and Re21 (Figs 3B and 3C, Figs
147 S3A and S3B). The number of PD-L1 positive cells was slightly increased by IFN γ treatment
148 in ISOS-1 whereas almost 100% of canine HSA cells expressed PD-L1 without IFN γ
149 treatment (Figs. 3B and C; Figs. S3A and 3B). Double staining of PD-L1 and Iba1 verified
150 that macrophages in ISOS-1 tumors and canine HSA cases expressed PD-L1 (Fig. 4A). Then,
151 we tested whether HSA tumor cells can induce PD-L1 expression in macrophages using
152 RAW264.7 cells. PD-L1 gene expression in RAW264.7 cells was induced by LPS and IFN γ
153 treatment (Fig. 4B). Furthermore, ISOS-1 conditioned medium significantly induced PD-L1
154 protein expression in RAW264.7 cells (Figs. 4C and 4D).

155 These results suggest that HSA evade immune attack through PD-L1 expression in
156 tumor cells and by inducing PD-L1 expression in macrophages.

157

158 **Discussion**

159 Here we demonstrated that a mouse HSA cell line, ISOS-1, can be used as a syngenic
160 model for HSA, and that macrophages are the major constituent of the HSA tumor
161 microenvironment in both ISOS-1 and canine HSA tumors. We also identified that ISOS-1
162 cells could recruit macrophages, polarize them to M2 macrophages, and induce PD-L1

163 expression in macrophages. In this study, we used two mouse HSA cell lines (ISOS-1 and
164 UV♀2) and one immortalized mouse endothelial cell line (LEII) as candidates of syngenic
165 models for canine HSA. As previous studies reported, ISOS-1 was the only mouse HSA cell
166 line that developed tumors in immunocompetent mice^{9,19}. ISOS-1 possessed similar molecular
167 features with canine HSA such as high KDM2B expression and similar expression patterns of
168 KDM2B targets whereas KDM2B was not highly expressed in UV♀2 and LEII. Based on these
169 results and our previous findings that KDM2B plays an important in canine HSA, it is highly likely
170 that KDM2B is a common factor for endothelial cell tumor malignancy.

171 We demonstrated that ISOS-1 cells recruited macrophages, polarized them to M2
172 macrophages, and induced PD-L1 expression in macrophages. In canine HSA tumors,
173 macrophages expressed both CD204⁺ and PD-L1, which suggests that canine HSA cells also
174 attract and induce macrophages to express PD-L1. Since T cells were located at the periphery
175 of canine HSA cases, macrophages in canine HSA likely facilitate immune evasion by through
176 induction of PD-L1 expression. Antibodies specific for canine PD-L1 have been developed
177 and have been tested for their safety and efficacy in clinical cases²⁰⁻²². However, anti-PD-L1
178 antibody treatment has not been studied in canine HSA patients. Given that more than 80% of
179 clinical HSA cases that we examined in our study expressed PD-L1 in tumor cells and/or
180 macrophages, immunotherapy using anti PD-L1 antibody treatment could be useful as an

181 alternative treatment for canine HSA. In our previous study, silencing of KDM2B resulted to
182 increased interferon gamma and alpha responses⁷. This means that KDM2B inhibition induces
183 immune reaction; therefore, combination therapy with anti-PD-L1 antibody and KDM2B
184 inhibition might provide better outcomes than single treatment with anti-PD-L1 or KDM2B
185 inhibitor treatment in canine HSA.

186 In summary, we identified the similarities between ISOS-1 and canine HSA, and we
187 demonstrated the usefulness of ISOS-1 as a syngeneic model for canine HSA. By taking
188 advantage of ISOS-1 cells, we characterized the tumor microenvironment in HSA and
189 demonstrated the crosstalk between tumor cells and macrophages for the induction of PD-L1
190 expression. These results provide useful insights for understanding HSA pathology and will be
191 beneficial to develop novel therapeutics for HSA.

192

193 **Materials and Methods**

194 *Cell lines*

195 ISOS-1 cells were obtained from the Cell Resource Center for Biomedical Research
196 Cell Bank (Tohoku University)⁹. UV♀2 cells were obtained from RIKEN Bioresource
197 Center¹⁰. The LEII cell line was donated by Dr. Kazuhiro Kimura (Hokkaido University) and
198 cultured as described previously^{23, 24}. RAW264.7 cells were obtained from RIKEN

199 Bioresource Center²⁵. Canine HSA cell lines (JuB2, JuB4, Re12, Ud6) were given by Dr.
200 Hiroki Sakai (Gifu University)²⁶. All cells used were routinely tested for *Mycoplasma* using
201 PCR and were submitted to ICLAS Monitoring Center (Kawasaki, Japan) for Mouse hepatitis
202 virus testing^{27, 28}.

203

204 ***Mouse lung endothelial cell isolation***

205 The primary mouse lung endothelial cell (MLEC) was isolated from a 10-week-old,
206 female, Balb/c mice and were cultured as described elsewhere²⁹. Briefly, freshly isolated
207 mouse lung were minced using autoclaved scissors, digested by collagenase I, and filtered
208 through a 70- μ m cell strainer. The cell suspension was incubated anti-rat Dynabeads (Thermo
209 Fisher Scientific) conjugated with anti-mouse CD31 antibody (BD Biosciences, NJ, USA,
210 557355). Pooled cells were seeded in a 12-well-plate pre-coated with 0.1% gelatin. Upon
211 reaching confluence, the cells were trypsinized and then incubated with anti-mouse ICAM-2
212 antibody (BD Biosciences, NJ, USA, 553326) conjugated Dynabeads. Pooled cells were
213 seeded in 12-well-plate pre-coated with 0.1% gelatin. Harvested cells were assessed using tube
214 formation assay, 1,1'-dioctadecyl-3,3,3',3'-tetramethyl-indocarbocyanine perchlorate Low
215 Density Lipoprotein (DiI-Ac-LDL) uptake, and CD31 gene expression (Figs. S4A - S4C).

216

217 ***Tube formation assay***

218 Tube formation was performed as described previously³⁰. Briefly, 1×10^5 JuB2 or
219 MLEC suspended in 24-hour JuB2 conditioned medium were seeded in a 24-well plate
220 pre-coated with Corning[®] Matrigel[®] Basement Membrane Matrix (Corning Inc. NY, USA).
221 Cells were observed at 0, 2, 4, and 8 hours after seeding for tube formation.

222

223 ***Dil-Ac-LDL uptake assay***

224 Dil-Ac-LDL uptake assay was performed with Dil-Ac-LDL staining kit (Cell
225 Applications, Inc.) according to the manufacturer's instructions. Briefly, 6×10^5 of isolated
226 MLEC were cultured in a 4-well chamber slide (Nunc Lab-Tek Chamber Slide System,
227 Thermo Fisher Scientific) precoated with Extracellular Matrix Attachment Solution provided
228 in the kit. MLEC were allowed to grow until 95% confluency. Culture medium from each
229 chamber was removed and cells were cultured in 100 μ L of culture medium supplemented
230 with 10 μ g/mL of Dil-Ac-LDL. Cells were incubated for 4 hours, washed with wash buffer,
231 and then mounted with DAPI-containing mounting medium and covered with 22 \times 50 mm
232 coverslip. Cells were examined under a confocal microscope (LSM700, Carl Zeiss,
233 Oberkochen, German).

234

235 ***Mice***

236 All mouse experiments were performed under the AAALAC guidelines in Hokkaido
237 University (protocol number:20-0083). Six-week-old male and female Balb/c mice purchased
238 from Japan SLC, Inc. (Shizuoka, Japan) were used as breeders for tumor transplantation
239 experiments. Mice were kept in a temperature-controlled specific-pathogen-free facility on a
240 12 hr light/dark cycle. Animals in all experimental groups were examined at least twice
241 weekly for tumorigenesis.

242

243 ***Tumor transplantation studies***

244 ISOS-1, LEII, and UV♀2 cell lines were cultured in 15 cm dishes accordingly. Mice
245 were randomly assigned to each group. 2×10^6 ISOS-1, LEII, or UV♀2 cells were
246 resuspended in Corning® Matrigel® Basement Membrane Matrix (Corning Inc. NY, USA) and
247 inoculated subcutaneously in mice anesthetized with 3% isoflurane. Tumor sizes were
248 measured twice weekly one week after inoculation. Mice were euthanized with CO₂ when
249 tumors reached 1,500 mm³ in volume or when mice exhibited abnormal behavior. Tumors
250 were fixed in 10% neutral buffered formalin and processed for routine histological
251 examination.

252

253 ***Cell viability analysis***

254 Cell viability after doxorubicin or GSK-J4 treatment was measured with Cell
255 Counting Kit-8 (Dojindo Molecular Technologies, Inc., Kumamoto, Japan) according to the
256 manufacturer's instructions. The absorbance at 450 nm was measured with NanoDrop™ 2000
257 (Thermo Fisher Scientific). Determination of IC₅₀ were performed using KyPlot 6.0 software
258 (KyensLab, Inc., Tokyo, Japan). Experiments were performed at least three times with
259 triplicates.

260

261 ***Western blotting***

262 Western blotting was performed as described previously⁷. The antibodies used in this
263 study are as follows: anti-KDM1A antibody (1:1000; Cell Signaling Technology, MA, USA,
264 2139S), anti-KDM2A antibody (1:1000; Abcam, Cambridge, UK, Ab191387), anti-KDM2B
265 antibody (1:1000; Santa Cruz Biotechnology, Inc., TX, USA, sc-293279), anti Actin antibody
266 (1:10000; Sigma Aldrich, MO, MAB1501), anti-c-FOS antibody (1:1000; Santa Cruz
267 Biotechnology, Inc., sc-166940), anti-γH2A.X antibody (1:1000; Bethyl Laboratories, Inc, TX,
268 USA, A300-081A-T), anti-p-ERK1/2 antibody (1:1000; Cell Signaling Technology, 4370S),
269 anti-ERK1/2 antibody (1:1000; Cell Signaling Technology, 4695S), anti-H2AK119Ub1
270 antibody (1:2000; Cell Signaling Technology-8240S), anti-H3 antibody (1:3000; MAB

271 Institute, Inc. Yokohama, Japan, MABI0001-20), and CD204 (1:125; Medicinal Chemistry
272 Pharmaceutical Co., Ltd., Sapporo, Japan, KT022). All primary antibodies were diluted in Can
273 Get Signal Solution[®] 1 (TOYOBO, Osaka, Japan). Membranes were washed with
274 Tris-Buffered Saline with 0.1% Tween[®] 20 (TBS-T) three times for 5 mins each time before
275 incubating with ECL Mouse IgG HRP-linked whole antibody (Cytiva, MA, USA, #NA934) or
276 ECL Rabbit IgG HRP-linked whole antibody (Cytiva, #NA931) diluted in Can Get Signal
277 Solution 2 (TOYOBO, Osaka, Japan). Signal development was performed using Immobilon[®]
278 Western Chemiluminescent HRP substrate (Merck Millipore, NJ, USA). ImageQuant LAS
279 4000 mini luminescent image analyzer (GE Healthcare) was used to visualize
280 chemiluminescent signals and the ImageJ software was used to process captured data³¹.

281

282 ***Quantitative RT-PCR (qRT-PCR)***

283 qRT-PCR was performed as described previously⁷. The list of primers used in this
284 study is listed in Supplementary table. cDNA of mouse mesenchymal stem cells (mMSC),
285 donated by Dr. Yusuke Komatsu (Hokkaido University), were used as a negative control for
286 *CD31* expression.

287

288 ***Flow cytometry analysis***

289 Flow cytometry for cell cycle was performed as described previously⁷. Briefly, $2 \times$
290 10^5 HSA cells were harvested for each replicate and unstained control. Samples were fixed
291 with 70% ethanol and incubated with propidium iodide (PI) in the dark for 30 mins at 37°C.
292 Unstained cells were incubated with PBS for 30 mins at 37°C. Cell cycle was analyzed in BD
293 FACSVerse™ flow cytometer (BD Biosciences, NJ, USA). Results were analyzed with FCS
294 Express 4 software (De Novo Software, CA, USA). Experiments were performed at least three
295 times with triplicates.

296 For PD-L1 expression analysis, HSA cells were cultured in 6-well plates until 90%
297 confluency. Cells were washed with 1.34 mM EDTA in PBS twice and then detached by
298 adding 1 mL of 1.34 mM EDTA solution and incubating at room temperature (RT) for 10-15
299 mins. Cells were counted and 2×10^5 cells were used for each replicate. Cells were blocked
300 with 10% goat serum in PBS with sodium azide at RT for 15 mins before incubating with anti
301 PD-L1 antibody (1:100; clone 6C11-3A11) or isotype rat IgG2a control (1:50; BD
302 Biosciences) at RT for 30 mins²¹. Cells were washed with 1% BSA in PBS twice before
303 incubating with secondary anti-rat IgG antibody conjugated with APC (1:500; Southern
304 Biotech, AL, USA, Catalog no. 3010-11L). Cells were analyzed in BD FACSVerse™ flow
305 cytometer (BD Biosciences, NJ, USA). Results were analyzed with FCS Express 4 software
306 (De Novo Software, CA, USA). Experiments were performed at least three times with

307 triplicates.

308

309 ***RAW264.7 polarization***

310 RAW264.7 cells were polarized to M1 or M2 macrophages as described by a

311 previous study³². 1×10^6 RAW264.7 cells were seeded in 10 cm dishes and were stimulated

312 with LPS (100 ng/ml) and IFN- γ (20 ng/ml) or TGF- β (10 ng/ml) for 24 hours for their

313 polarization towards the M1 or M2 subtype, respectively. RAW264.7 cells were also incubated

314 in 48 hour-conditioned medium from ISOS-1 cell culture filtered with a 0.45 μ m sterile filter.

315 RAW264.7 cells cultured under normal DMEM medium were considered as M0 or

316 unpolarized macrophages.

317

318 ***Transwell migration assay***

319 Migration assay for RAW264.7 cells was performed as described previously with

320 minor changes³³. Briefly, 2.5×10^5 RAW264.7 cells in 1 mL normal medium were added to

321 ThinCerts cell culture inserts (Greiner Bio-One, Kremsmünster, Austria) in 6 well plates while

322 2.5 mL of 48 hours conditioned medium from MLEC or ISOS-1 cells were added to the lower

323 wells. After 24 hours, cells in the upper wells were removed with a cotton swab, filters were

324 fixed with 4% paraformaldehyde in PBS and stained with 0.1% crystal violet solution in DW.

325 Cell migration was assessed by counting the number of migrated cells in five fields per well at
326 40× magnification.

327

328 ***Histopathological analysis and Immunohistochemistry***

329 Tissue samples were fixed for at least 48 hours in 10% neutral buffered formalin,
330 processed routinely, embedded in paraffin, and sectioned 3 μm thick, mounted on glass slides,
331 and stained with hematoxylin and eosin (HE). All tumors were examined for KDM2B
332 expression and presence of lymphocytes and macrophages using immunohistochemistry (IHC).
333 IHC was performed using antibodies to Iba1 (1:2000, Fujifilm Wako, Osaka, Japan,
334 019-19741), CD3 (1:1000; Agilent Technologies, CA, USA, IR503), KDM2B (1:50; Santa
335 Cruz Biotechnology, Inc., sc-293279), CD31 (1:250; Abcam, JC/70A), PD-L1 (1:100; clone
336 6C11-3A11), and CD204 (1:800; Medicinal Chemistry Pharmaceutical Co., Ltd., Sapporo,
337 Japan, KT022) as described previously⁷. Nano Zoomer 2.0-RS (Hamamatsu Photonics,
338 Hamamatsu, Japan) was used to scan histological slides, which were then processed in QuPath
339 ver 0.2.133³⁴. Scanned slides were opened in QuPath as Brightfield (H-DAB), and the
340 Estimate Stain Vectors feature was used to automatically adjust the staining colors. Normal
341 endothelial and tumor cells were detected using the Cell Detection function. The Create
342 Detection Classifiers function was used to label cells based on their morphologies and

343 locations, allowing the QuPath software to correctly classify each cell type. The collected data
344 was exported and used for further analysis.

345

346 ***Immunofluorescence assay***

347 Tissue samples were fixed, processed, and incubated with primary antibodies for
348 Iba1 and PD-L1 as described above. Tissue samples were washed with PBS three times for 5
349 minutes each before adding a secondary goat anti-rabbit IgG H & L (1:1000, Alexa Fluor®
350 555, Abcam) and Goat Anti-Rat IgG H & L (1:1000, Alexa Fluor® 488, Abcam) in 5% skim
351 milk for 1 hour at RT. Sections were washed with PBS three times for 5 mins each, mounted
352 with DAPI-containing mounting medium, and covered with 24 × 32 mm coverslip. Tissues
353 were examined under a confocal microscope (LSM700, Carl Zeiss, Oberkochen, German).

354

355 ***Statistical analysis***

356 Statistical analyses were performed with Microsoft Excel and R software (version
357 3.6.3). Student's *t*-test was used to analyze the difference between two groups while Tukey's
358 test was used to analyze differences between multiple groups. *P*-values less than 0.05 were
359 considered statistically significant.

360

361 **Data availability**

362 The datasets generated during and/or analyzed during the current study are available from the
363 corresponding author on reasonable request.

364

365 **References**

- 366 1. Spangler, W. L. & Culbertson, M. R. Prevalence, type, and importance of
367 splenic diseases in dogs: 1,480 cases (1985-1989). *J Am Vet Med Assoc* **200**,
368 829–834 (1992).
- 369 2. Prymak, C., McKee, L. J., Goldschmidt, M. H. & Glickman, L. T.
370 Epidemiologic, clinical, pathologic, and prognostic characteristics of splenic
371 hemangiosarcoma and splenic hematoma in dogs: 217 cases (1985). *J Am Vet Med*
372 *Assoc* **193**, 706–712 (1988).
- 373 3. Johannes, C. M. *et al.* Hemangiosarcoma in cats: 53 cases (1992-2002). *J*
374 *Am Vet Med Assoc* **231**, 1851–1856 (2007).
- 375 4. Sastry, G. A. Angiosarcoma (hemangioendothelioma) in the thorax of a
376 mule. *Vet Rec* **63**, 145–147 (1951).
- 377 5. Shimizu, H., Nagel, D. & Toth, B. Ethylhydrazine hydrochloride as a
378 tumor inducer in mice. *Int J Cancer* **13**, 500–505 (1974).
- 379 6. Young, R. J., Brown, N. J., Reed, M. W., Hughes, D. & Woll, P. J.
380 Angiosarcoma. *Lancet Oncol* **11**, 983–991 (2010).
- 381 7. Montecillo Gulay, K. C. *et al.* KDM2B promotes cell viability by enhancing
382 DNA damage response in canine hemangiosarcoma. *Journal of Genetics and*
383 *Genomics* (2021) doi:10.1016/j.jgg.2021.02.005.
- 384 8. Azmi, A. & Mohammad, R. M. *Animal Models in Cancer Drug Discovery*.
385 (Academic Press, 2019).
- 386 9. Masuzawa, M. *et al.* Establishment of a new murine phenotypic
387 angiosarcoma cell line (ISOS-1). *Journal of Dermatological Science* **16**, 91–98
388 (1998).
- 389 10. Toda, K. *et al.* Establishment and characterization of a tumorigenic
390 murine vascular endothelial cell line (F-2). *Cancer Res* **50**, 5526–5530 (1990).
- 391 11. Allavena, P., Sica, A., Garlanda, C. & Mantovani, A. The Yin-Yang of

- 392 tumor-associated macrophages in neoplastic progression and immune surveillance.
393 *Immunol Rev* **222**, 155–161 (2008).
- 394 12. Chen, Y. *et al.* Tumor-associated macrophages: an accomplice in solid
395 tumor progression. *Journal of Biomedical Science* **26**, 78 (2019).
- 396 13. Wang, Y. & Harris, D. C. H. Macrophages in renal disease. *J Am Soc*
397 *Nephrol* **22**, 21–27 (2011).
- 398 14. Kaku, Y. *et al.* M2 macrophage marker CD163, CD204 and CD206
399 expression on alveolar macrophages in the lung of patients with chronic
400 obstructive pulmonary. *European Respiratory Journal* **44**, (2014).
- 401 15. Hashimoto, R. *et al.* LPS enhances expression of CD204 through the
402 MAPK/ERK pathway in murine bone marrow macrophages. *Atherosclerosis* **266**,
403 167–175 (2017).
- 404 16. Lescoat, A. *et al.* M1/M2 polarisation state of M-CSF blood-derived
405 macrophages in systemic sclerosis. *Annals of the Rheumatic Diseases* **78**,
406 e127–e127 (2019).
- 407 17. Nagano, M. *et al.* CD204-positive macrophages accumulate in breast
408 cancer tumors with high levels of infiltrating lymphocytes and programmed death
409 ligand-1 expression. *Oncol Lett* **21**, 36 (2021).
- 410 18. Kubota, K. *et al.* CD163+CD204+ tumor-associated macrophages
411 contribute to T cell regulation via interleukin-10 and PD-L1 production in oral
412 squamous cell carcinoma. *Sci Rep* **7**, 1755 (2017).
- 413 19. Kitajima, T., Iwashiro, M., Kuribayashi, K. & Imamura, S. Immunological
414 characterization of tumor-rejection antigens on ultraviolet-light-induced tumors
415 originating in the CB6F1 mouse. *Cancer Immunol Immunother* **38**, 372–378
416 (1994).
- 417 20. Maekawa, N. *et al.* Immunohistochemical Analysis of PD-L1 Expression
418 in Canine Malignant Cancers and PD-1 Expression on Lymphocytes in Canine
419 Oral Melanoma. *PLoS One* **11**, e0157176 (2016).
- 420 21. Maekawa, N. *et al.* A canine chimeric monoclonal antibody targeting
421 PD-L1 and its clinical efficacy in canine oral malignant melanoma or
422 undifferentiated sarcoma. *Sci Rep* **7**, 8951 (2017).
- 423 22. Maekawa, N. *et al.* PD-L1 immunohistochemistry for canine cancers and
424 clinical benefit of anti-PD-L1 antibody in dogs with pulmonary metastatic oral
425 malignant melanoma. *npj Precis. Onc* **5**, 1–9 (2021).
- 426 23. Kitamura, T. *et al.* Proinsulin C-peptide activates cAMP response
427 element-binding proteins through the p38 mitogen-activated protein kinase

- 428 pathway in mouse lung capillary endothelial cells. *Biochem J* **366**, 737–744 (2002).
- 429 24. Curtis, A. S. G. & Renshaw, R. M. Lymphocyte-Endothelial Interactions
430 and Histocompatibility Restriction. in *In Vivo Immunology: Histophysiology of the*
431 *Lymphoid System* (eds. Nieuwenhuis, P., van den Broek, A. A. & Hanna, M. G.)
432 193–198 (Springer US, 1982). doi:10.1007/978-1-4684-9066-4_26.
- 433 25. Raschke, W. C., Baird, S., Ralph, P. & Nakoinz, I. Functional macrophage
434 cell lines transformed by abelson leukemia virus. *Cell* **15**, 261–267 (1978).
- 435 26. Murai, A. *et al.* Constitutive phosphorylation of the mTORC2/Akt/4E-BP1
436 pathway in newly derived canine hemangiosarcoma cell lines. *BMC Veterinary*
437 *Research* **8**, 128 (2012).
- 438 27. Harasawa, R. *et al.* Detection and tentative identification of dominant
439 mycoplasma species in cell cultures by restriction analysis of the 16S-23S rRNA
440 intergenic spacer regions. *Res. Microbiol.* **144**, 489–493 (1993).
- 441 28. Harasawa, R. *et al.* Rapid detection and differentiation of the major
442 mycoplasma contaminants in cell cultures using real-time PCR with SYBR Green
443 I and melting curve analysis. *Microbiol. Immunol.* **49**, 859–863 (2005).
- 444 30. DeCicco-Skinner, K. L. *et al.* Endothelial Cell Tube Formation Assay for
445 the In Vitro Study of Angiogenesis. *J Vis Exp* (2014) doi:10.3791/51312.
- 446 31. Schneider, C. A., Rasband, W. S. & Eliceiri, K. W. NIH Image to ImageJ:
447 25 years of image analysis. *Nat. Methods* **9**, 671–675 (2012).
- 448 32. Vidyarthi, A. *et al.* TLR-3 Stimulation Skews M2 Macrophages to M1
449 Through IFN- $\alpha\beta$ Signaling and Restricts Tumor Progression. *Front. Immunol.* **9**,
450 (2018).
- 451 33. Chen, Y. *et al.* SAK-HV Promotes RAW264.7 cells Migration Mediated by
452 MCP-1 via JNK and NF- κ B Pathways. *Int J Biol Sci* **14**, 1993–2002 (2018).
- 453 34. Bankhead, P. *et al.* QuPath: Open source software for digital pathology
454 image analysis. *Scientific Reports* **7**, 16878 (2017).

455

456

457 **Acknowledgments**

458 We would like to extend our sincerest gratitude to Dr. Kazuhiro Kimura (Hokkaido
459 University) and Dr. Hiroki Sakai (Gifu University) for providing LEII cell line and canine

460 hemangiosarcoma cell lines, respectively. We are grateful to the members of the Laboratory of
461 Comparative Pathology, Faculty of Veterinary Medicine, Hokkaido University for their
462 invaluable support during the conduct of this study. This research was supported by the
463 KAKENHI Grant-in-Aid for Young Scientist (KA, 20K15654) provided by Japan Society for
464 the Promotion of Science, and by a research grant provided by the Kuribayashi Foundation
465 (KA, No. 2-2)

466

467 **Author contributions**

468 **K. G.** Conceptualization, Methodology, Investigation, Formal Analysis, Data Curation,
469 Writing - Original Draft, Writing - Review & Editing, **K. A.** Conceptualization, Writing -
470 Review & Editing, Supervision, Funding acquisition. **N. M.** and **S. K.** Methodology and
471 supervision. **A. K.** Writing - Review & Editing. **T.K.** Supervision.

472

473 **Conflict of Interest Statement**

474 The authors declared no potential competing conflicts of interests with respect to the research,
475 authorship or, and publication of this article.

476

477 **Figure legends**

478

479 **Fig. 1. ISOS-1 presents similar morphology and molecular features with canine HSA.**

480 **A**, Hematoxylin and eosin (HE) staining in ISOS-1 and canine HSA tumors. **B**, KDM1A,
481 KDM2A, and KDM2B protein expressions in MLEC, ISOS1, LEII, and UV♀2 cell lines. **C**,
482 KDM2B immunohistochemistry of ISOS-1 and canine HSA tumors. **D**, Histograms of PI
483 intensities in ISOS1, LEII, and UV♀2 cell lines. **E**, Percentages of cells with aneuploidy in
484 ISOS1, LEII, and UV♀2 cell lines. **F**, Western blotting for phosphorylated ERK1/2
485 (p-ERK1/2), c-FOS, γ H2A.X and H2AK119ub1 in MLEC, ISOS-1, LEII, and UV♀2 cell lines.
486 **G**, Quantification of p-ERK1/2, c-FOS, γ H2A.X, and H2AK119ub1 in MLEC, ISOS-1, LEII,
487 and UV♀2 cell lines. p-ERK1/2 expression was normalized with total ERK1/2 expression.
488 c-FOS expression was normalized with Actin expression. H2AK119Ub1 and γ H2A.X
489 expressions were normalized with H3 expression levels. The protein expression levels in
490 MLEC were set to 1. Data are presented as mean values \pm s.d. Experiments were performed in
491 triplicates. Scale = 125 μ m. *** $P < 0.001$, Tukey's test.

492

493 **Fig. 2 HSA cells attract macrophages and polarize them to M2 macrophages.**

494 **A**, HE staining and immunohistochemistry of CD3 and Iba1 for ISOS-1 and canine HSA
495 tumors. **B**, Quantitative analysis of Iba1 positive cells in ISOS-1 and canine HSA tumors.

496 Y-axis indicates the percentages of Iba1 positive cells relative to all cells comprising the tumor
497 tissue. **C**, Transwell migration assay in RAW264.7 cells cultured over MLEC- or
498 ISOS-1-conditioned media. **D**, Quantitative analysis of **C**. **E**, Gene expressions of M1 or M2
499 macrophage markers in untreated, LPS and IFN-treated, TGF β -treated, and ISOS-1
500 conditioned media-treated RAW264.7 cells. **F**, (Left) Western blot analysis for CD204 in
501 untreated, LPS and IFN-treated, TGF β -treated, and ISOS1 conditioned media-treated
502 RAW264.7 cells. (Right) Quantitative analysis of the western blotting data. **G**,
503 Immunohistochemistry of CD204 for ISOS-1 and canine HSA tumors. Scale = 125 μ m. Data
504 are presented as mean values \pm s.d.

505

506 **Fig. 3 HSA cells express PD-L1.**

507 **A**, HE staining and immunohistochemistry of PD-L1 for ISOS-1 and canine HSA tumors. HE
508 staining images are the same as in Fig. 2A because the same samples were used for this
509 experiment. **B**, Representative images of flow cytometry analysis for PD-L1 in ISOS-1 and
510 JuB2 cell lines with/without IFN γ treatment. APC indicates PD-L1 expressions. **C**,
511 Quantitative analysis of **B**. Scale = 125 μ m. Data are presented as mean values \pm s.d. *** $P <$
512 0.001, Tukey's test.

513

514 **Fig. 4 ISOS-1 cells induce PD-L1 expression in RAW264.7 cells.**

515 **A**, Immunofluorescence assay for PD-L1 and Iba1 in ISOS-1 and canine HSA tumors. Arrows

516 indicate the cells expressing both PD-L1 and Iba1. **B**, Gene expression levels of PD-L1 in

517 untreated, LPS and IFN-treated, TGF β -treated, and ISOS-1 conditioned media-treated

518 RAW264.7 cells. **C**, Representative images of flow cytometry analysis for PD-L1 in

519 RAW264.7 cells cultured in normal or ISOS-1 conditioned media. **D**, Quantitative analysis of

520 C. Data are presented as mean values \pm s.d. *** $P < 0.001$, Tukey's test.

521

522

523 **Table**

524 PD-L1 expression in tumor and immune cells in canine HSA.

Patient No.	Sex	Age (years)	Breed	PD-L1 intensity (tumor cells)	PD-L1 intensity (macrophages)	PD-L1 intensity (lymphocytes)
1	Male (castrated)	7	Miniature Dachshund	-	+++	-
2	Female (spayed)	7	Golden Retriever	+	-	-
3	Male	14	Miniature Schnauzer	-	-	-
4	Female (spayed)	10	Mixed	+	+++	-
5	Male (castrated)	12	Beagle	+	-	-
6	Male	8	Labrador Retriever	++	+++	-
7	Female (spayed)	10	Miniature Dachshund	++	+++	-
8	Female (spayed)	14	Miniature Dachshund	-	+++	-
9	Female (spayed)	14	Miniature Schnauzer	-	-	-
10	Male (castrated)	12	Miniature Schnauzer	+	+++	-
11	Male	13	French Bulldog	-	-	-
12	Male (castrated)	14	Miniature Dachshund	-	+++	-
13	Female (spayed)	12	Labrador Retriever	-	+++	-
14	Male (castrated)	14	Lhasa Apso	+	-	-
15	Female (spayed)	12	Beagle	-	+++	-
16	Female (spayed)	14	Miniature Dachshund	+	+++	-
17	Male (castrated)	14	Miniature Dachshund	++	+++	-
18	Female	8	Flat-coated Retriever	-	+++	-
19	Female (spayed)	11	Scottish Terrier	++	+++	-
20	Female	5	Golden Retriever	++	+++	-
21	Male	5	Beagle	++	+++	-
22	Female	9	Golden Retriever	+	-	-
23	Male	10	Miniature Schnauzer	++	+++	-
24	Female	12	Mixed	-	-	-
25	Male	9	Great Pyrenees	-	+++	-
26	Male	7	Jack Russel Terrier	-	-	-
27	Male (castrated)	8	Labrador Retriever	-	+++	-
28	Male (castrated)	10	Maltese	+	+++	-

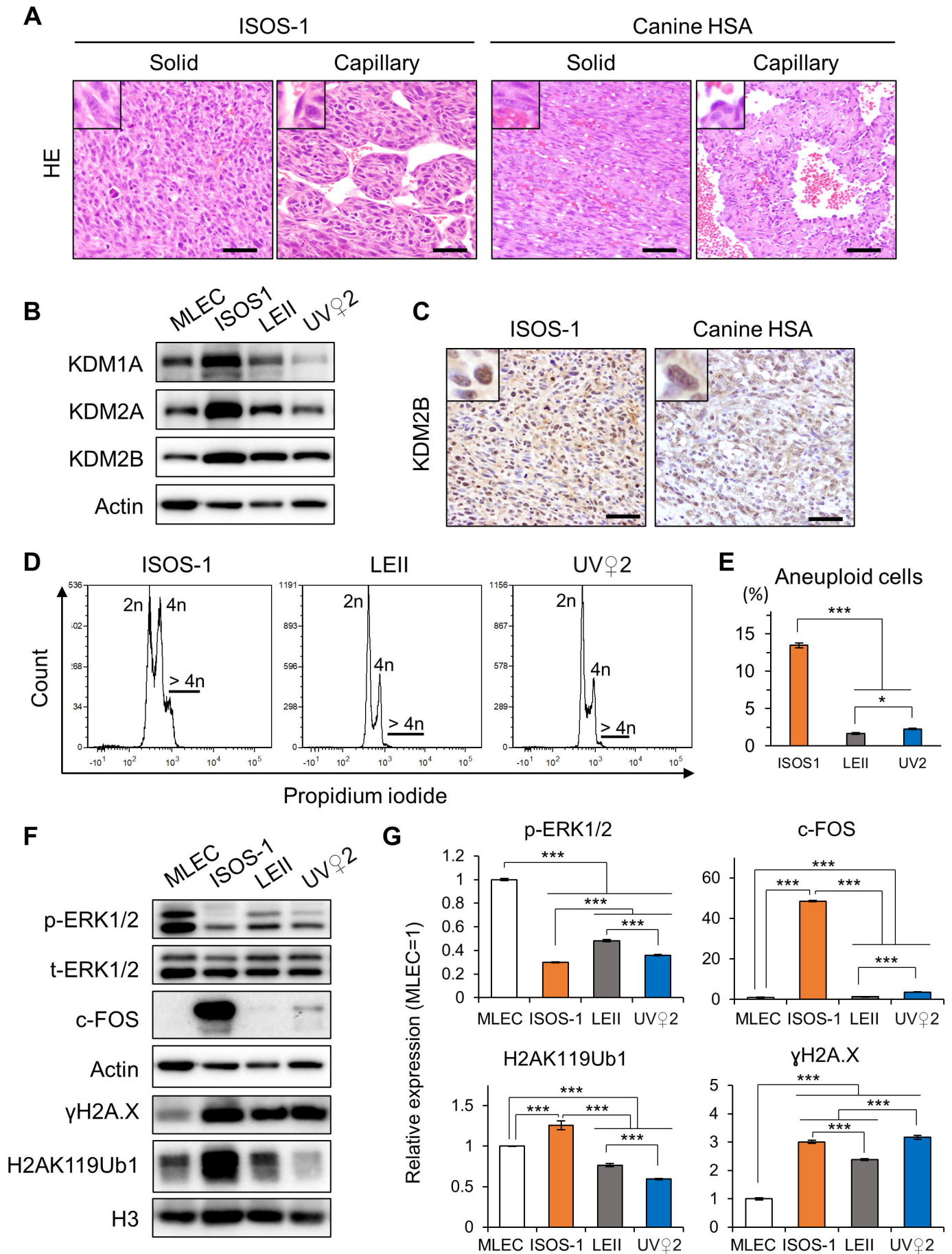


Fig. 1

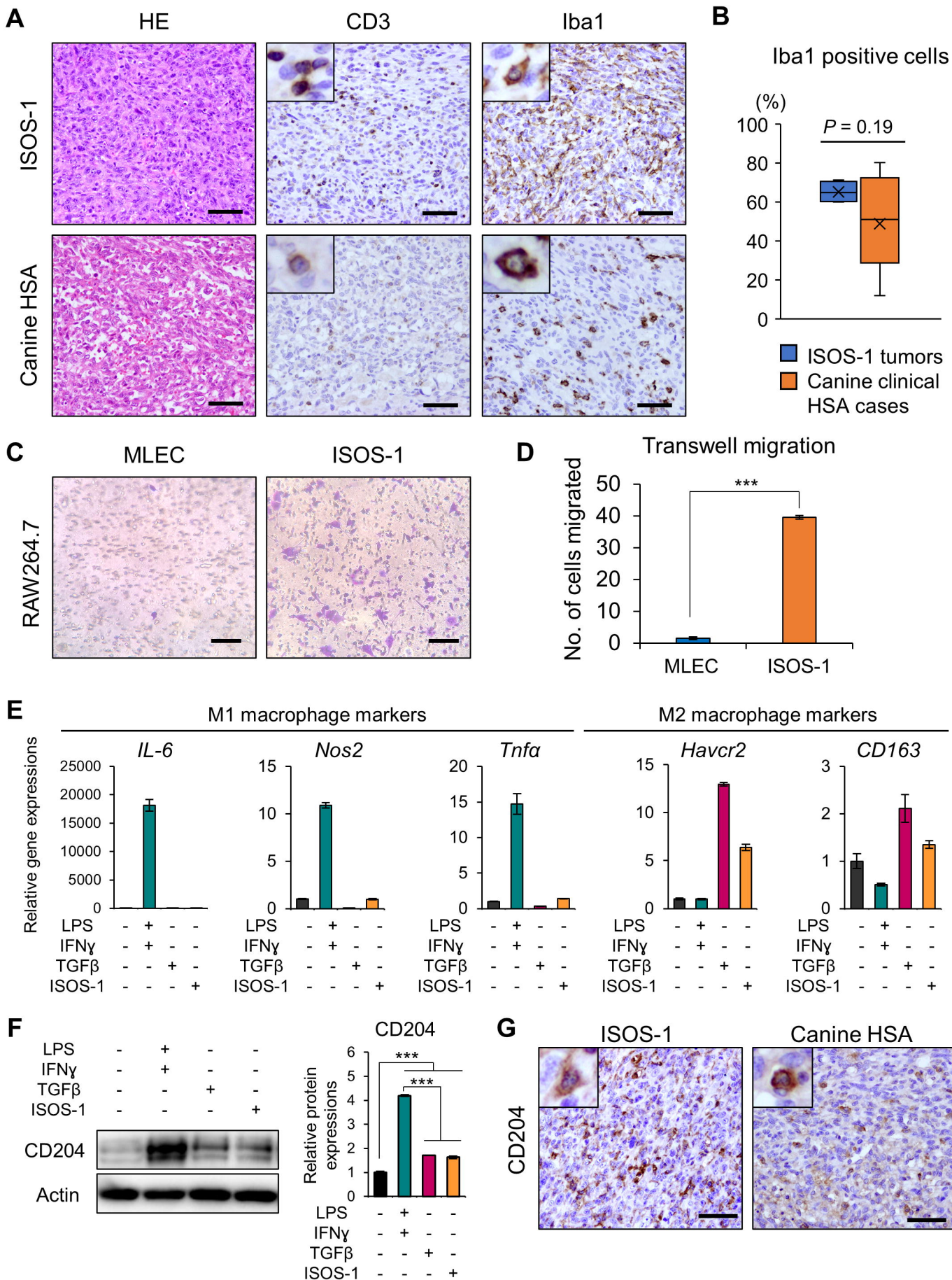


Fig. 2

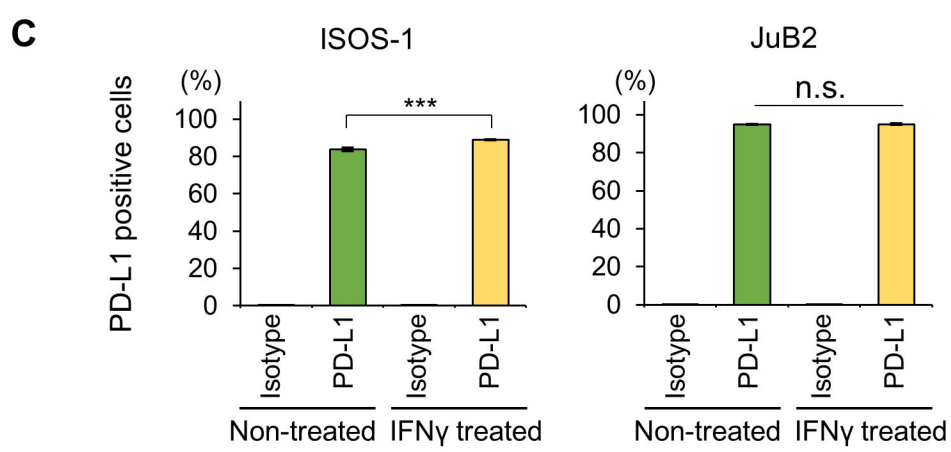
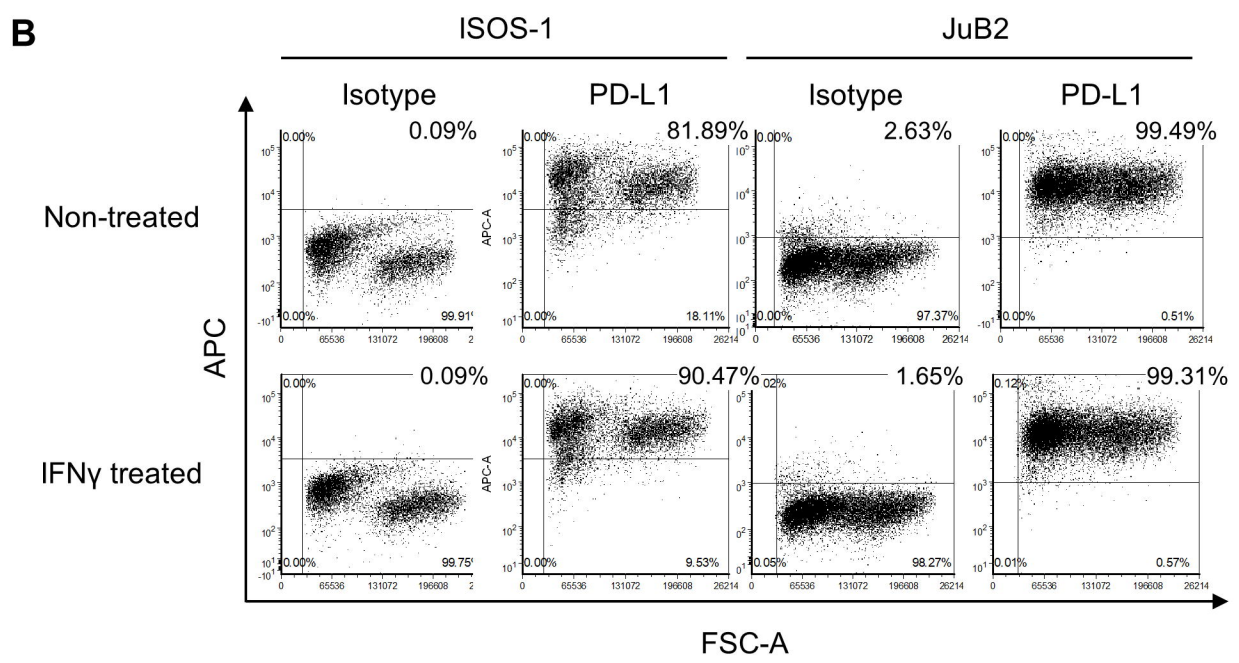
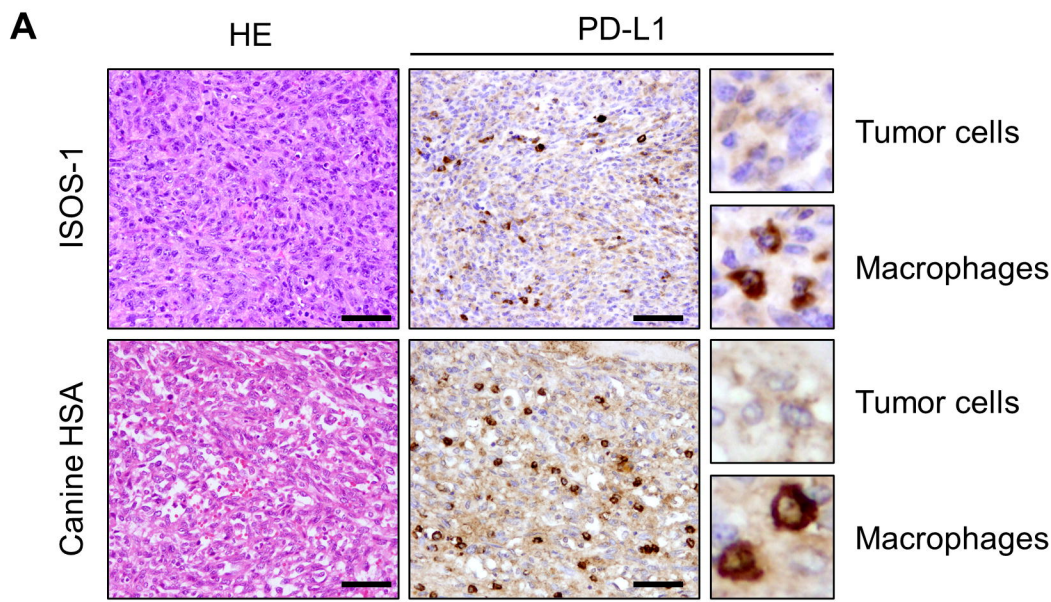


Fig. 3

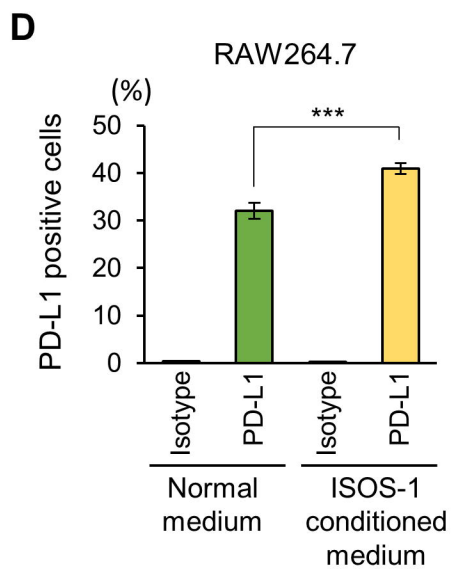
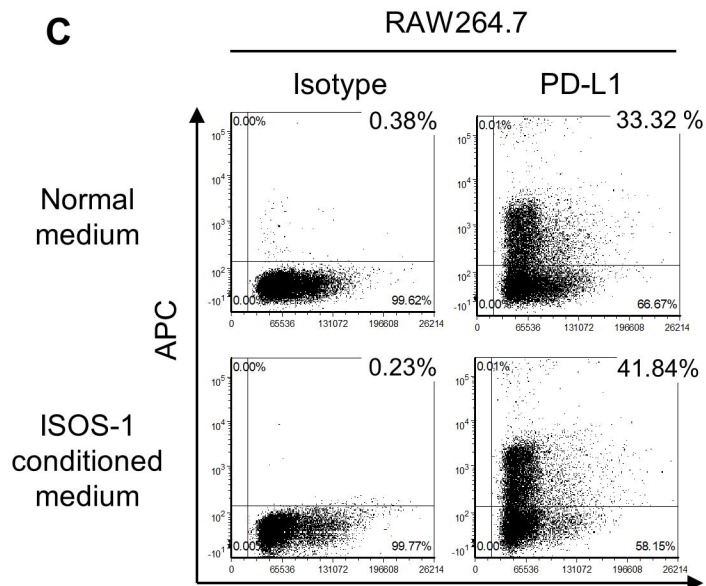
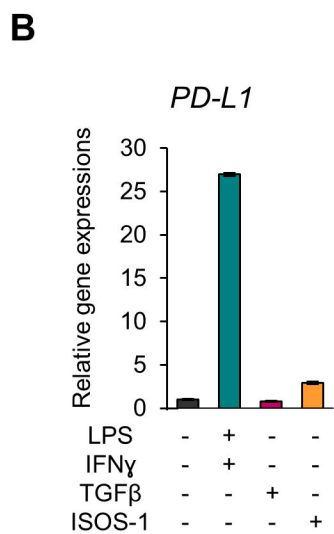
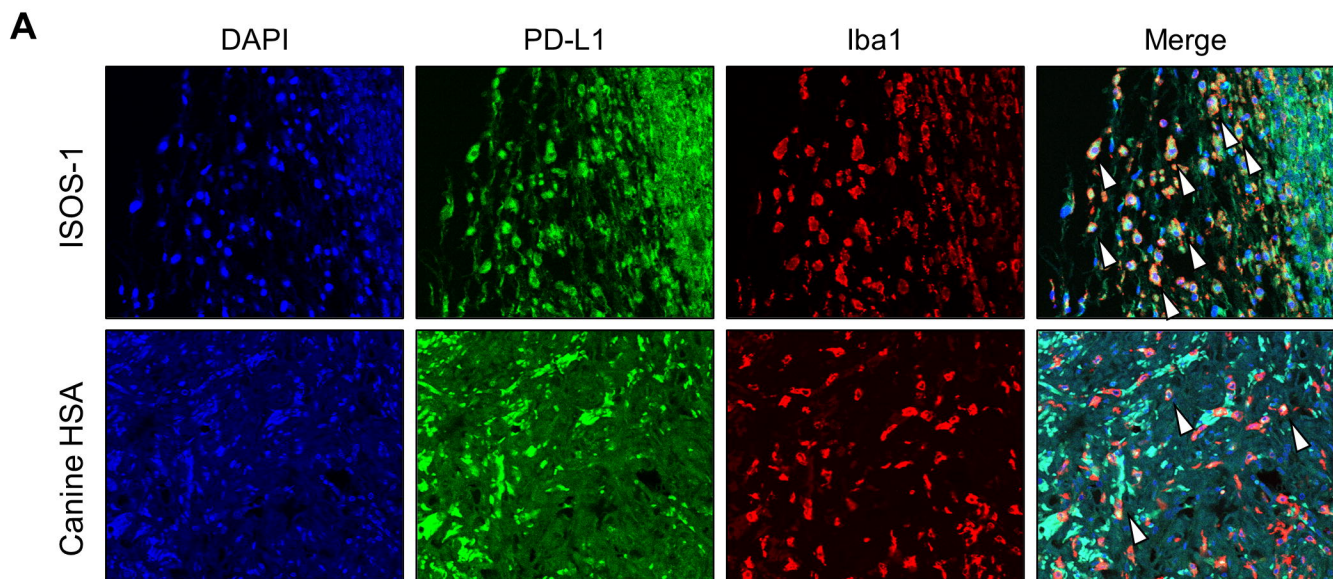


Fig. 4